Geophysical Research Letters

RESEARCH LETTER
10.1029/2019GL084789

Leveraging the Rapid Retreat of the Amundsen Gulf Ice Stream 13,000 Years Ago to Reveal Insight Into North American Deglaciation

T. Pico[1,2], A. Robel[3], E. Powell[1], A. C. Mix[4], and J. X. Mitrovica[1]

[1]Department of Earth & Planetary Sciences, Harvard University, Cambridge, MA, USA, [2]Division of Geological and Planetary Sciences, Caltech, Pasadena, CA, USA, [3]School of Earth & Atmospheric Sciences, Georgia Tech, Atlanta, GA, USA, [4]College of Earth, Ocean, and Atmospheric Sciences, Oregon State University, Corvallis, OR, USA

Key Points:
- Ice streams are sensitive to history of deglaciation
- We use ice stream collapse to differentiate between proposed deglacial ice histories

Supporting Information:
- Supporting Information S1

Correspondence to:
T. Pico,
tpico@caltech.edu

Citation:
Pico, T., Robel, A., Powell, E., Mix, A. C., & Mitrovica, J. X. (2019). Leveraging the rapid retreat of the Amundsen Gulf Ice Stream 13,000 years ago to reveal insight into North American deglaciation. *Geophysical Research Letters*, *46*. https://doi.org/10.1029/2019GL084789

Received 1 AUG 2019
Accepted 1 OCT 2019
Accepted article online 16 OCT 2019

Abstract We examine the influence of different deglacial histories of the North American ice saddle, which connected the Cordilleran ice sheet and western Laurentide ice sheet, on the stability of the fast-flowing Amundsen Gulf Ice Stream, located in the northwestern Laurentide ice sheet. We use a simplified marine-terminating ice stream model to simulate grounding line retreat and compare our predictions to geologic evidence for the rapid collapse of the Amundsen Gulf Ice Stream at 13 ka. We show that observations of ice stream retreat can be used to distinguish between past ice unloading histories, and that the rapid retreat of the Amundsen Gulf Ice Stream near 13 ka is most dynamically consistent with substantial deglaciation of the North American ice saddle from 13 to 11.5 ka, during the Younger Dryas cooling episode. These results suggest that short-lived changes in ice stream behavior may be used to reveal larger-scale and longer-duration ice sheet dynamics.

1. Introduction

1.1. Amundsen Gulf Ice Stream

The Amundsen Gulf, in the Canadian Arctic Archipelago, was formerly occupied by a thick ice stream. Evidence for this past ice stream was originally based on the geomorphology of topographic depressions and was later mapped by satellite, marine, multibeam imagery,(Maclean et al., 2015) and seismic reflection profiles.(Batchelor et al., 2014) The ice stream was a drain for the northwestern Laurentide ice sheet (LIS). As a conduit of freshwater and sediment supply to the Arctic Ocean,(Batchelor et al., 2014) the ice stream may have played an important role in ice-ocean-climate interactions over the last deglaciation (26 to 11.7 ka[3]). Over much of this period, ice streams of the northwestern LIS terminated in the Arctic Ocean, at times flowing over reverse-sloped bedrock (deepening toward the ice sheet interior), similar to present-day Antarctic ice streams.(Joughin & Alley, 2011)

Evidence from the geological record helps to constrain the dynamics of the Amundsen Gulf Ice Stream. Scours from the former Amundsen Gulf Ice Stream have been identified and used to map ice extent over time.(Maclean et al., 2015; Stokes et al., 2006) Furze et al.,(Furze et al., 2017) presented evidence of a former ice shelf in the eastern Northwest Passage (east of the Amundsen Gulf Ice Stream), which may have stabilized the retreating LIS margin until 12.5 ka. A recent study suggested a freshwater event in the Arctic at 12.8 ka was sourced from a rapid retreat of the Amundsen Gulf Ice Stream (250 km of retreat in less than 500 years), based on dated ice rafted debris (cores 44PC and 56 PC) and seismic reflection profiles. (Lakeman et al., 2018)

1.2. Marine Ice Sheet Instability

The stability of marine-terminating ice streams is strongly sensitive to the slope of underlying bedrock. (Schoof, 2007) A marine ice sheet instability occurs when the grounding line retreats on a reverse-sloped bed, which results in a greater ice mass flux (that increases nonlinearly with bed depth at the grounding line), and fuels additional retreat. In formerly glaciated regions, bedrock topography (and therefore changes in slope) is strongly modulated by the time-dependent glacial isostatic adjustment (GIA) of the crust.(Gomez et al., 2010) The dynamics of former marine-terminating ice streams were therefore sensitive to changes in bed slope that occurred in response to prior variations in the regional ice thickness.

1.3. Timing of Ice Unloading

Evidence for the timing and rapid retreat of the Amundsen Gulf Ice Stream at 12.8 ka(Lakeman et al., 2018) motivates our model investigation of North American deglacial ice histories because ice sheet dynamics depend on bedrock topography. This topography is, in turn, controlled by the history of previous ice cover. While the timing and source of ice melt from North America during the last deglaciation can be constrained by tracking the age of retreat of past ice margins, as well as the timing of freshwater flux to the oceans in sedimentary cores(Menounos et al., 2017)$^{-15}$, these methods do not provide a direct measure of past ice thickness. Records of ice stream retreat can provide insight into past ice thickness because the stability of the ice stream depends on bedrock slope changes induced by GIA, and these changes are ultimately governed by ice sheet volume, rather than ice margin locations.

In some reconstructions of North American deglaciation, the ice saddle connecting the Laurentide (LIS) and Cordilleran (CIS) ice sheets is assumed to have melted primarily during Meltwater Pulse 1a (MWP-1a; 14.5 ka(Deschamps et al., 2012)). For example, an ice sheet modeling study(Gregoire et al., 2012) predicted a rapid collapse of the ice saddle equivalent to a global mean sea level (GMSL) rise of ~10.5 m in 0.5 ky and connected this event to MWP-1a, though the modeled event did not match the timing of MWP-1a inferred from sea level records. The global ice model ICE-6G sources a large contribution to MWP-1a from a rapid ice thinning between the CIS and LIS equivalent to 6.9 m GMSL from 14.5 to 14 ka.(Peltier & Fairbanks, 2006)

A recent study has modified ICE-6G to delay this substantial melt of the saddle at 14.5 ka until 13 ka in order to reconcile sea level constraints imposed by the two-phased flooding history of the Bering Strait.(Pico et al., 2018) In this proposed ice history (GI-31), substantial melting occurs from 13 to 11.5 ka. The difference in timing and rates of unloading in the saddle region between the ICE-6G and GI-31 ice histories would drive different GIA signals and retrodicted paleotopographies at 13 ka in the Amundsen Gulf Ice Stream region. In the GI-31 ice history, there is a persistent regional ice load until 13 ka, which causes a more depressed bed in the interior and greater reverse slopes near the ice margin at 13 ka relative to the ICE-6G case.

Here we combine a simple numerical model for the evolution of a marine-terminating glacier to simulate the migration of the Amundsen Gulf Ice Stream grounding line position with a model of GIA-induced sea level to test the consistency of the above ice loading histories with ice stream retreat rates observed in the geologic record.(Lakeman et al., 2018) Notably, we show that certain models of ice sheet deglaciation are more dynamically consistent with observed geologic evidence for rapid ice stream retreat.

2. Methods

2.1. GIA Modeling

The decay of ice sheets across the last deglaciation drove a complex spatiotemporal pattern of sea level change due to deformational, gravitational, and rotational effects of GIA. Our simulations are based on the sea level theory and pseudospectral algorithm described by Kendall et al.(Kendall et al., 2005) at a spherical harmonic truncation at degree and order 256. This treatment includes the impact of load-induced Earth rotation changes on sea level,(Milne & Mitrovica, 1996) evolving shorelines and the migration of grounded, marine-based ice.(Johnston, 1993; Kendall et al., 2005; Lambeck et al., 2003; Milne et al., 1999) These predictions require models for Earth's viscoelastic structure and the spatiotemporal history of ice cover.

For the first of these, we adopt a mantle viscosity profile based on a GIA analysis of local sea level records in our region of interest.(Gowan et al., 2016) Specifically, the Earth model is characterized by a lithospheric thickness of 96 km and an upper and lower mantle viscosities of 4×10^{20} and 10^{22} Pa s, respectively. We perform sensitivity tests by varying these values to show that our results are insensitive to this choice. Paleobedrock topography at 13 ka is calculated by subtracting the computed spatial field of sea level change from modern-day topography.

As we have noted, ICE-6G(Peltier et al., 2015) is characterized by a rapid loss of ice mass in the saddle region (Cordilleran and western Laurentide) equivalent to 6.9-m GMSL from 14.5 to 14 ka. The model sources additional meltwater from this region from 14 to 13 ka, equivalent to 3.7-m GMSL. GI-31 was constructed by modifying the deglaciation geometry of the ICE-6G model while requiring that the total ice volume (or GMSL) history of that model be preserved to satisfy far-field sea level constraints.(Pico et al., 2018) The

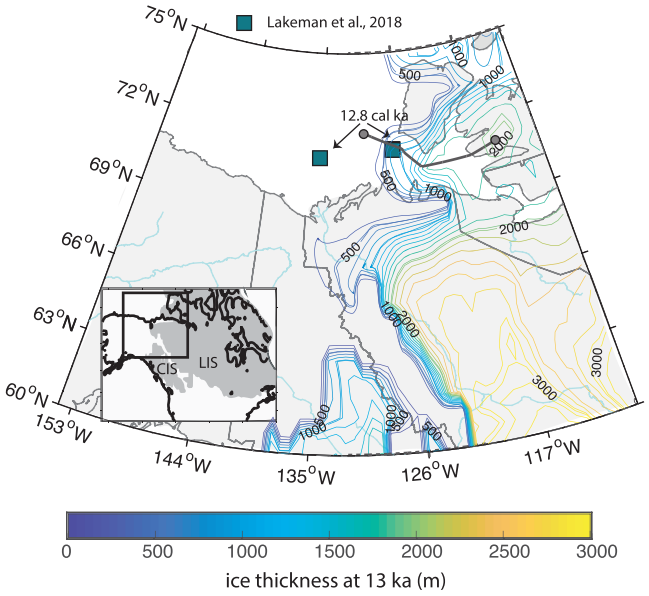

Figure 1. Location and age of sites that constrain the timing of ice rafted debris and freshwater influx.(Lakeman et al., 2018) Contours show ice thickness at 13 ka in the GI-31 ice history. Transect of Amundsen Gulf Ice Stream used in simulations is shown by the dark gray line. Inset shows location of Cordilleran (CIS) and Laurentide (LIS) ice margins at 13 ka in the GI-31 ice history.

GI-31 ice history is characterized by a melting of the ice saddle equivalent to 14.3-m GMSL from 13 to 11.5 ka.(Pico et al., 2018) Since the GI-31 history is based on deglacial snapshots of the ICE-6G model, the two histories are characterized by the same pattern of deglaciation; however, they differ in the timing and rate of ice melt.

2.2. Marine-Terminating Ice Stream Model

The glaciological properties (such as basal friction, degree of buttressing, or surface accumulation rate) of the Amundsen Gulf Ice Stream at 13 ka are poorly constrained. Thus, to simulate a range of possible retreat histories for this ice stream, we use a simple two-equation model that captures the essential aspects of evolving marine-terminating ice stream dynamics and accumulation rate with a minimum of parameters.(Robel et al., 2018) The model, described in detail in supporting information, reconstructs the temporal evolution of grounding line position and the spatially averaged ice stream thickness.(Robel et al., 2018) At time scales longer than a few decades, it is an excellent approximation of the grounding line migration predicted in spatially extended ice stream models. (Robel et al., 2018) Thus, it is an ideal tool to efficiently simulate the multicentennial migration of the Amundsen Gulf Ice Stream at 13 ka with a given paleotopography, under a wide range of parameter values.

We predicted paleotopography by calculating GIA associated with the GI-31 ice history. We used the two-equation marine-terminating glacier model, initiated at 13 ka, to calculate the evolution of the grounding line and therefore, retreat rates, of the Amundsen Gulf Ice Stream. We adopted the ice thickness and paleo-bedrock profile associated with the GI-31 history at 13 ka (transect in Figure 2; Figure 3a) as the initial conditions.

The two-equation model requires values for the spatially averaged surface accumulation rate, degree of buttressing from an ice shelf, and friction between ice and the underlying topography. We varied these parametric values and densely sampled the corresponding parameter space. Specifically, we varied the friction coefficient from 1×10^6 to 6×10^6 Pa $m^{-1/3}$ $s^{-1/3}$, the buttressing coefficient (which we label as θ) from 0.5 to 1 (strongly buttressed to no buttressing at the grounding line), and the accumulation rate from 0.1 to 0.3 m/year, consistent with previous estimates of regional accumulation rate at this time.(Ullman et al., 2015) This parameter sweep resulted in 1,000 distinct simulations.

3. Results

3.1. Paleotopography

Figure 2 shows ice thickness and the solid Earth elevation at 13 ka retrodicted using the ICE-6G and GI-31 models. Figure 3b plots profiles of paleo-bedrock topography (or paleotopography) at 13 ka across these two fields along a transect through the former position of the Amundsen Gulf Ice Stream (Figures 1 and 2). A bedrock sill is located ~180 km upstream of the initial ice stream margin.

The difference in the profiles in Figure 3b is shown in Figure 3c. The average bedrock slope underlying the Amundsen Gulf Ice Stream over the 250-km segment upstream of the initial grounding line position is 1.816 m/km for the prediction based on the ice model GI-31 and 1.560 m/km for the ICE-6G simulation. A steeper retrograde slope is predicted on the GI-31 simulation because the interior region has greater isostatic depression at this time due to the more persistent local ice cover. We note that the ice stream has disappeared in the ICE-6G simulation by 13 ka.

3.2. Ice Stream Retreat

We predicted the evolution of grounding line retreat of the Amundsen Gulf Ice Stream beginning at 13 ka over a period of 500 years (gray lines in Figure 4a). We found that 210 of 1,000 simulations predicted a total grounding line retreat of 250 km or more over the 500-year simulation (Figure 4b).

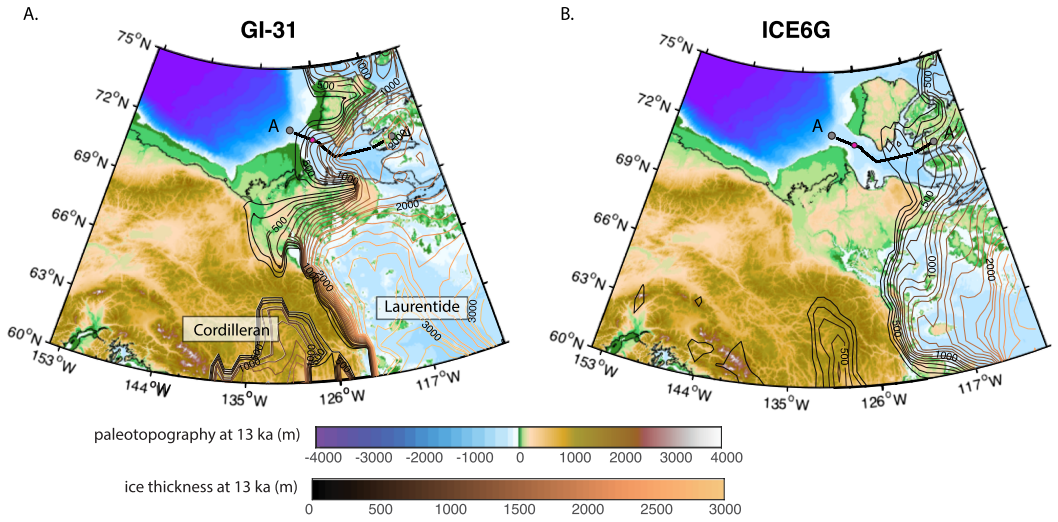

Figure 2. Paleo topography at 13 ka computed using ice histories GI-31 (a) and ICE-6G (b). Ice thickness for each history is shown by colored contours. The dark blue line from A to A′ shows the transect through the Amundsen Gulf Ice Stream used in the ice stream simulations described in the text. Black contours show the present-day shoreline. Magenta dot shows location of sill in Figure 3b.

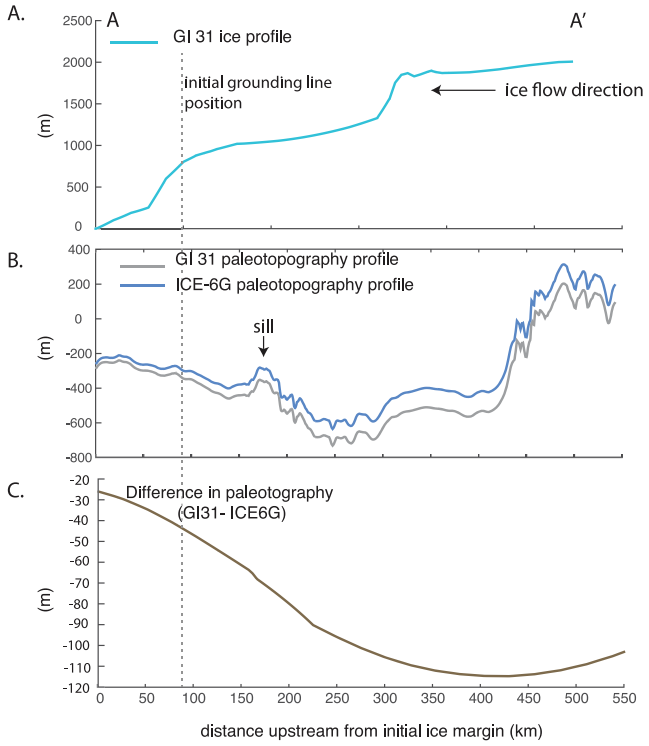

Figure 3. (a) Amundsen Gulf Ice Stream thickness at 13 ka in the GI-31 ice history (transect shown in Figures 1 and 2). In the ICE-6G history, the ice stream has disappeared by 13 ka. Paleotopography across the same transect at 13 ka for simulations based on GI-31 (gray) and ICE-6G (blue). (c) Difference in paleotopographies in frame B. The initial grounding line position adopted in the simulations is shown by the vertical dashed gray line (~85 km upstream from initial ice margin). Note that the ice margin and grounding line positions are different because there is floating ice.

Histograms showing values of the three parameters that resulted in a total retreat of more than 250 km are shown in Figure 5. A rapid retreat of the Amundsen Gulf Ice Stream on the GI-31 paleotopography is not predicted in the cases of small friction coefficients ($< 2 \times 10^6$ Pa $m^{-1/3}$ $s^{-1/3}$) or a high degree of buttressing ($\theta < 0.8$). However, a rapid retreat was possible for the full range of accumulation rates we considered (0.1–0.3 m/year).

Over the simulation time window (13–12.5 ka), the unloading of ice from the retreating Amundsen Gulf Ice Stream, in addition to melting ice in the saddle region, caused isostatic rebound, which may have prevented grounding line retreat. Since our simulations did not evolve topography over the 500 years modeled, we investigated whether the time-dependent isostatic adjustment of the crust would have prevented grounding line retreat. We performed simulations that used the same range of parameter values in Figure 4 and the GI-31 ice profile in Figure 3a but adopted the paleotopography associated with the GI-31 history at 12.5 ka (rather than 13 ka), the end of our simulation time interval. In this case, we found that 190/1,000 simulations produced over 250 km of grounding line retreat within 500 years (supporting information Figure S1). Therefore, crustal rebound from 13 to 12.5 ka only slightly reduces the set of parameter sets consistent with rapid retreat. That is, despite some crustal rebound from melting ice, the paleotopography at 12.5 ka had not experienced sufficient uplift to impede extensive (>250 km) retreat of the ice stream.

4. Discussion

Approximately one fifth of the simulations based on paleotopography computed using the GI-31 ice history resulted in rates of ice stream retreat consistent with the observed retreat in the geologic record. Assuming that the simple marine-terminating ice stream model we have adopted is representative of conditions at 13 ka close to the Amundsen Gulf Ice Stream, we can use the results of our simulations

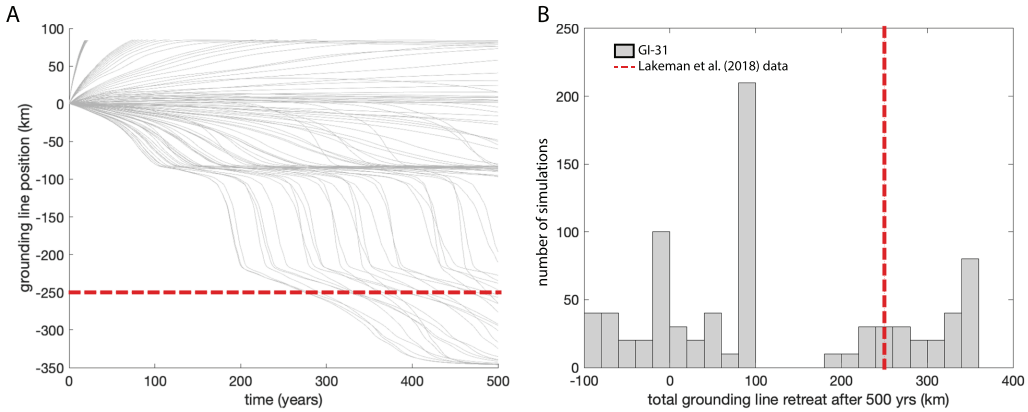

Figure 4. (a). Grounding line position (relative to the initial position) calculated from the marine-terminating glacier model using the GI-31 (gray) paleotopography. (b) Histogram showing the number of simulations (of 1,000 total) predicting specific ranges of grounding line retreat after 500 years. The dotted red line is the total grounding line retreat of the Amundsen Gulf Ice Stream reported by Lakeman et al. (2018); reaching this retreat extent with our model runs requires ~300 years or longer.

to infer glaciologic conditions. Specifically, the simulations that satisfied constraints on ice stream retreat required a high buttressing coefficient θ (corresponding to a low degree of buttressing) and a relatively high friction coefficient, suggesting that the ice stream was not significantly buttressed and that it was underlain by regolith.

We also explored the sensitivity of our results to the choice of Earth model adopted in GIA simulations. We repeated the calculations in Figures 4–6 using an alternate Earth model characterized by a lithospheric thickness of 48 km and an upper and lower mantle viscosities of 5×10^{20} and 5×10^{21} Pa s, respectively, consistent with previous inferences of mantle viscosity profiles based on GIA data sets.(Lambeck et al., 1998; Mitrovica & Forte, 2004) We found that the number of simulations that produced a retreat of the ice stream of more than 250 km in 500 years remained precisely the same—210—although the timing and total retreat distance varied from those obtained in the main results (supporting information Figure S2).

We next performed ice stream simulations using the ice thickness of the Amundsen Gulf Ice Stream in ICE-6G at 14.5 ka (Figure 2b) and the associated GIA-corrected paleotopography at this time. With the same range of parameter sets adopted in Figure 4, we found that 350/1,000 simulations for ICE-6G at 14.5 ka predict over 250 km of grounding line retreat within 500 years (supporting information Figure S3). These results suggest that, at 14.5 ka, paleotopography was sufficiently isostatically depressed to allow the grounding line to retreat past the sill ~180 km upstream of the initial ice margin. However, this timing for rapid retreat of the Amundsen Gulf Ice Stream is inconsistent with geologic evidence documenting the collapse of this ice stream at 13 ka.

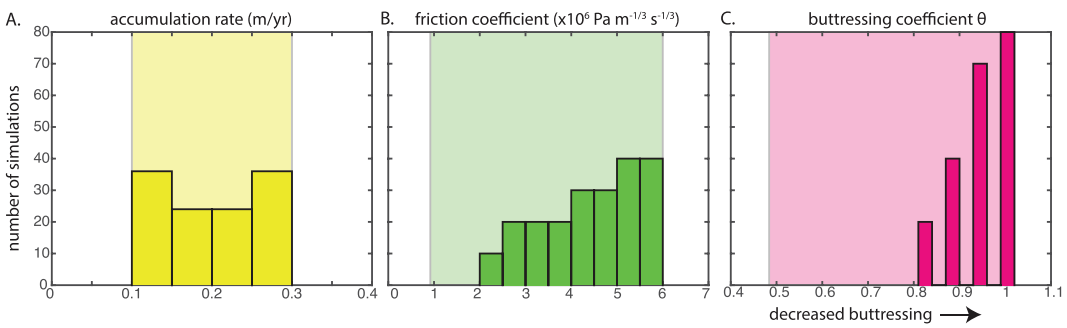

Figure 5. Histogram showing parameters (a, accumulation rate; b, friction coefficient in Pa $m^{-1/3}$ $s^{-1/3}$; and c, buttressing coefficient) that produce a total grounding line retreat of over 250 km using the GI 31 paleotopography predicted using the GI-31 ice history. Shaded regions represent the range of parameters explored.

As an additional sensitivity test, we performed simulations adopting the ice profile in GI-31 at 13 ka (Figure 3a) and the paleotopography associated with ICE-6G at 13 ka (Figure 3b, blue). In contrast to simulations using GI-31, none of the 1,000 based on the ICE-6G paleotopography predicted a total grounding line retreat of more than 100 km (supporting information Figure S4, blue). This result illustrates well the sensitivity of ice stream retreat to bedrock topography. Correcting topography for GIA using these two ice histories produces different paleotopographies and therefore different bedrock slopes underlying the Amundsen Gulf Ice Stream. Specifically, along the Amundsen Gulf Ice Stream transect, the ICE-6G paleotopography is 50- to 100-m higher than the GI-31 paleotopography at 13 ka. Ice stream simulations based on the GI-31 ice thickness at 13 ka and reconstructed bed topographies using the GI-31 and ICE-6G are characterized by much lower ice flux at the grounding line in latter case. Indeed, the computed ice flux when the ICE-6G reconstruction of topography is adopted is sufficiently low to prevent the ice stream from retreating past the bedrock sill upstream from the initial ice margin. This sill represents a critical gatekeeper for unstable retreat in this area.

4.1. Implications for Younger Dryas

Freshwater discharge into the Arctic has been hypothesized to have slowed the Atlantic Meridional Overturning Circulation and triggered the Younger Dryas cooling episode.(Broecker & Denton, 1989; Tarasov & Peltier, 2005; Tarasov & Peltier, 2006) Evidence for a meltwater pulse event has been discovered in geochemical and geologic signals of sediment core records(Andrews & Dunhill, 2004; Deschamps et al., 2018; Keigwin et al., 2018; Klotsko et al., 2019; Spielhagen et al., 2005) and on-land geologic evidence of flooding,(Murton et al., 2010) although the freshwater volume and flux rate have not been quantified. Spielhagen et al. (2005) observed a freshwater peak in Siberian Arctic sediment cores near 13 cal ka. In the Canadian Arctic, a freshwater peak is similarly observed near the Mackenzie Delta from 12.7 to 11.6 cal ka in core P189AR-P45(Andrews & Dunhill, 2004) and from 12.9 to 12.2 cal ka in core HLY1302-JPC15,27,9.(Keigwin et al., 2018)

This body of evidence has been used to argue that a catastrophic flood sourced from Glacial Lake Agassiz brought large volumes of freshwater to the Arctic via the northern proto-Mackenzie drainage(Keigwin et al., 2018) and/or North Atlantic via the southern Laurentian drainage. (Leydet et al., 2018) Lakeman et al.,(Lakeman et al., 2018) in contrast, suggested that the retreat of the Amundsen Gulf Ice Stream, as indicated by seismic reflection data and ice rafted debris, could have been the source of a large flux of freshwater at this time. In particular, they inferred a minimum of 250 km of ice stream retreat in less than 500 years and invoked the marine ice sheet instability as a mechanism for the event. Our simulations based on ice history GI-31 support their suggestion that ice stream retreat played a role in the flux of freshwater into the Arctic at 13 ka.

5. Conclusion

Our analysis demonstrates that evidence of past ice stream dynamics may provide a new tool for inferring ice loading histories. Since the stability of ice streams is sensitive to underlying bedrock slope, and bedrock slopes are sensitive to local ice history, evidence of past ice stream collapse has the potential to impose important physical constraints on the history of deglaciation.

We used a simple ice flow model and different paleotopographies retrodicted using a GIA-based sea level theory to demonstrate that the rapid retreat of the Amundsen Gulf Ice Stream at 13 ka inferred by Lakeman et al.(Lakeman et al., 2018) is dynamically consistent with substantial melting of the saddle region between the Cordilleran and the western LIS from 13 to 11.5 ka. The timing of deglaciation of the saddle region strongly modulates the stability of any nearby marine-terminating ice streams and therefore also has an important control on the timing of freshwater influx into the Arctic and the associated climatic response.

Our results are consistent with independent evidence for a large freshwater flux into the Arctic during the Younger Dryas and lend support to the hypothesis that this freshwater is sourced, at least in part, from a melting ice sheet in addition to outburst flooding. Additional analyses of geochemical proxies in sediment core records may aid in refining constraints on the timing and source of freshwater into the Arctic during the Younger Dryas.

Acknowledgments

T.P. acknowledges funding from Harvard University and NSF-GRFP. Ice models used for this research are available at PANGAEA, a publicly accessible online repository, at https://issues.pangaea.de/browse/PDI-21803.

References

Andrews, J. T., & Dunhill, G. (2004). Early to mid-Holocene Atlantic water influx and deglacial meltwater events, Beaufort Sea slope, Arctic Ocean. *Quaternary Research*, *61*, 14–21.

Batchelor, C. L., Dowdeswell, J. A., & Pietras, J. T. (2014). Evidence for multiple Quaternary ice advances and fan development from the Amundsen Gulf cross-shelf trough and slope, Canadian Beaufort Sea margin. *Marine and Petroleum Geology*, *52*, 125–143.

Broecker, W. S., & Denton, G. H. (1989). The role of ocean-atmosphere reorganizations in glacial cycles. *Geochimica et Cosmochimica Acta*, *53*, 2465–2501.

Deschamps, C., Montero-Serrano, J. C., & Stonge, G. (2018). Sediment provenance changes in the western Arctic Ocean in response to ice rafting, sea level, and oceanic circulation variations since the last deglaciation. *Geochemistry, Geophysics, Geosystems*, *19*, 2147–2165. https://doi.org/10.1029/2017GC007411

Deschamps, P., Durand, N., Bard, E., Hamelin, B., Camoin, G., Thomas, A. L., et al. (2012). Ice-sheet collapse and sea-level rise at the Bølling warming 14, 600 years ago. *Nature*, *483*(7391), 559–564. https://doi.org/10.1038/nature10902

Furze, M. F. A., Pienkowski, A. J., Mcneely, M. A., Bennett, R., & Cage, A. G. (2017). Deglaciation and ice shelf development at the northeast margin of the Laurentide ice sheet during the Younger Dryas chronozone. *Boreas*, *47*(1), 271–296. https://doi.org/10.1111/bor.12265

Gomez, N., Mitrovica, J. X., Huybers, P., & Clark, P. U. (2010). Sea level as a stabilizing factor for marine-ice-sheet grounding lines. *Nature Geoscience*, *3*(12), 580. https://doi.org/10.1038/NGEO1012

Gowan, E. J., Tregoning, P., Purcell, A., Montillet, J., & Mcclusky, S. (2016). A model of the western Laurentide ice sheet, using observations of glacial isostatic adjustment. *Quaternary Science Reviews*, *139*, 1–16.

Gregoire, L. J., Payne, A. J., & Valdes, P. J. (2012). Deglacial rapid sea level rises caused by ice-sheet saddle collapses. *Nature*, *487*(7406), 219–222. https://doi.org/10.1038/nature11257

Johnston, P. (1993). The effect of spatially non-uniform water loads on prediction of sea-level change. *Geophysical Journal International*, *114*, 615–634.

Joughin, I., & Alley, R. B. (2011). Stability of the west Antarctic ice sheet in a warming world. *Nature Geoscience*, *4*, 506–513.

Keigwin, L. D., Klotsko, S., Zhao, N., Reilly, B., Giosan, L., & Driscoll, N. W. (2018). Deglacial floods in the Beaufort Sea preceded Younger Dryas cooling. *Nature Geoscience*, *11*(8), 599–604. https://doi.org/10.1038/s41561-018-0169-6

Kendall, R. A., Mitrovica, J. X., & Milne, G. A. (2005). On post-glacial sea level - II. Numerical formulation and comparative results on spherically symmetric models. *Geophysical Journal International*, *161*, 679–706.

Klotsko, S., Driscoll, N., & Keigwin, L. (2019). Multiple meltwater discharge and ice rafting events recorded in the deglacial sediments along the Beaufort Margin, Arctic Ocean. *Quaternary Science Reviews*, *203*, 185–208.

Lakeman, T. R., Pieńkowski, A. J., Nixon, F. C., Furze, M. F. A., Blasco, S., Andrews, J. T., & King, E. L. (2018). Collapse of a marine-based ice stream during the early Younger Dryas chronozone, western Canadian Arctic. *Geology*, *46*(3), 211–214. https://doi.org/10.1130/G39665.1

Lambeck, K., Purcell, A., Johnston, P., Nakada, M., & Yokoyama, Y. (2003). Water-load definition in the glacio-hydro-isostatic sea-level equation. *Quaternary Science Reviews*, *22*, 309–318.

Lambeck, K., Smither, C., & Johnston, P. (1998). Sea-level change, glacial rebound and mantle viscosity for northern Europe. *Geophysical Journal International*, *134*(1), 102–144. https://doi.org/10.1046/j.1365-246x.1998.00541.x

Leydet, D. J., Carlson, A. E., Teller, J. T., Breckenridge, A., Barth, A. M., Ullman, D. J., et al. (2018). Opening of glacial Lake Agassiz's eastern outlets by the start of the Younger Dryas cold period. *Geology*, *46*(2), 155–158. https://doi.org/10.1130/G39501.1

Maclean, B., Blasco, S., Bennett, R., Lakeman, T., Hughes-Clarke, J., Kuus, P., & Patton, E. (2015). New marine evidence for a Late Wisconsinan ice stream in Amundsen Gulf, Arctic Canada. *Quaternary Science Reviews*, *114*, 149–166. https://doi.org/10.1016/j.quascirev.2015.02.003

Menounos, B., Goehring, B. M., Osborn, G., Margold, M., Ward, B., Bond, J., et al. (2017). Cordilleran ice sheet mass loss preceded climate reversals near the Pleistocene termination. *Science*, *358*(6364), 781–784. https://doi.org/10.1126/science.aan3001

Milne, G. A., & Mitrovica, J. X. (1996). Postglacial sea-level change on a rotating Earth: First results from a gravitationally self-consistent sea-level equation. *Geophysical Journal International*, *126*, F13–F20.

Milne, G. A., Mitrovica, J. X., & Davis, J. L. (1999). Near-field hydro-isostasy: The implementation of a revised sea-level equation. *Geophysical Journal International*, *139*, 464–482.

Mitrovica, J. X., & Forte, A. M. (2004). A new inference of mantle viscosity based upon joint inversion of convection and glacial isostatic adjustment data. *Earth and Planetary Science Letters*, *225*, 177–189.

Murton, J. B., Bateman, M. D., Dallimore, S. R., Teller, J. T., & Yang, Z. (2010). Identification of Younger Dryas outburst flood path from Lake Agassiz to the Arctic Ocean. *Nature*, *464*.

Peltier, W. R., Argus, D. F., & Drummond, R. (2015). Space geodesy constrains ice age terminal deglaciation: The global ICE-6G_C (VM5a) model. *Journal of Geophysical Research: Solid Earth*, *120*, 450–487. https://doi.org/10.1002/2014JB011176

Peltier, W. R., & Fairbanks, R. G. (2006). Global glacial ice volume and Last Glacial Maximum duration from an extended Barbados sea level record. *Quaternary Science Reviews*, *25*, 3322–3337.

Pico, T., Mitrovica, J. X. & Mix, A. C. Two-phase flooding of the Bering Strait reflects the sea-level fingerprint of an expanding ice-free corridor. Science Advances (2018)

Robel, A. A., Roe, G. H., & Haseloff, M. (2018). Response of marine-terminating glaciers to forcing: Time scales, sensitivities, instabilities and stochastic dynamics. *Journal of Geophysical Research: Earth Surface*, *123*, 2205–2227. https://doi.org/10.1029/2018JF004709

Schoof, C. (2007). Ice sheet grounding line dynamics: Steady states, stability, and hysteresis. *Journal of Geophysical Research*, *112*, F03S28. https://doi.org/10.1029/2006JF000664

Spielhagen, R. F., Erlenkeuser, H., & Siegert, C. (2005). History of freshwater runoff across the Laptev Sea (Arctic) during the last deglaciation. *Global and Planetary Change*, *48*, 187–207.

Stokes, C. R., Clark, C. D., Winsborrow, M. C. M., & Sea, B. (2006). Subglacial bedform evidence for a major palaeo-ice stream and its retreat phases in Amundsen Gulf. *Canadian Arctic Archipelago*, *21*, 399–412.

Tarasov, L., & Peltier, W. R. (2005). Arctic freshwater forcing of the Younger Dryas cold reversal. *Nature*, *435*, 662–665.

Tarasov, L., & Peltier, W. R. (2006). A calibrated deglacial drainage chronology for the North American continent: Evidence of an Arctic trigger for the Younger Dryas. *Quaternary Science Reviews*, *25*, 659–688.

Ullman, D. J., Carlson, A. E., Anslow, F. S., Legrande, A. N., & Licciardi, J. M. (2015). Laurentide ice-sheet instability during the last deglaciation. *Nature Geoscience*, *8*, 534–537.